Prepared for submission to JHEP

Einstein Equations from Information-Geometric Variational Principle: A Rigorous Derivation with Explicit Commutable Limit and Radon-Type Closure

Haobo Ma[1] **Wenlin Zhang**[2]

[1] *Independent Researcher*

[2] *National University of Singapore*

E-mail: aloning@gmail.com, e1327962@u.nus.edu

Abstract: We derive the local Einstein equations for $d \geq 3$ from an information-geometric variational principle on small causal diamonds. Under scale separation and absence of conjugate points, the first-order stationarity of the generalized entropy

$$S_{\rm gen} = \frac{A}{4G\hbar} + S_{\rm out}^{\rm ren} + S_{\rm ct}^{\rm UV} - \frac{\Lambda}{8\pi G}\frac{V}{T}$$

with a fixed-volume constraint implies $R_{kk} = 8\pi G\, T_{kk}$ via an explicit area–curvature balance and a weighted null ray transform. A tensorial closure then yields $G_{ab} + \Lambda g_{ab} = 8\pi G\, T_{ab}$. The second-order layer provides stability: $\delta^2 S_{\rm rel} = \mathcal{E}_{\rm can} \geq 0$ when the JLMS/$\mathcal{F}_Q$ identification applies. Appendix M supplies three ingredients used in the main text: a uniform modular-Hamiltonian approximation with a half-space–to–diamond kernel comparison, local invertibility and stability of the first-moment null ray transform, and a local construction of weak-shear diamonds with C^2 stability. Global density of weak-shear families in generic C^3 backgrounds remains open.

Keywords: Information-geometric variational principle, Einstein equations, Generalized entropy, Causal diamond, Raychaudhuri equation, Null energy condition, Hollands–Wald canonical energy, Covariant phase space, Fisher–Rao metric, KMS condition

Contents

---

1 Notation, Domain Prerequisites and Quick Reference

Notation and units: Metric signature $(-,+,+,+)$; $c = k_B = 1$, retain $\hbar$. Einstein tensor $G_{ab} = R_{ab} - \frac{1}{2}Rg_{ab}$. Null contraction $R_{kk} := R_{ab}k^a k^b$, $T_{kk} := T_{ab}k^a k^b$. **Volume and area:** Let **waist hypersurface** Σ_ℓ be the maximal spatial cross-section of causal diamond $\mathcal{D}_\ell$ (dimension $d{-}1$), with volume $V(B_\ell) := \mathrm{Vol}(\Sigma_\ell)$; let **waist surface** $\partial\Sigma_\ell$ be its boundary (dimension $d{-}2$), with area $A := \mathrm{Area}(\partial\Sigma_\ell)$. Denote $B_\ell := \Sigma_\ell$, $S_\ell := \partial B_\ell$ (waist surface); below dA always refers to the intrinsic measure on S_ℓ; leading-order scaling $A \sim c_d \ell^{d-2}$ (constant absorbed into C_d).

Domain prerequisites: Scale separation $\varepsilon_{\mathrm{curv}} = \ell/L_{\mathrm{curv}}$, $\varepsilon_{\mathrm{mat}} = \ell/L_{\mathrm{mat}}$, $\varepsilon = \max(\varepsilon_{\mathrm{curv}}, \varepsilon_{\mathrm{mat}}) \ll 1$; Hadamard-class state and point-splitting renormalization; in small interval $[0, \lambda_*]$ **no conjugate/focal points** (Sachs/Raychaudhuri controllable, ray transform locally invertible).

Invariants quick reference (invariant under rescaling $k^a \to \alpha k^a$, $\lambda \to \lambda/\alpha$, $\kappa \to \alpha\kappa$ and orientation flip):

$$\frac{\delta Q}{T} = \frac{2\pi}{\hbar}\int_{\mathcal{H}} \lambda\, T_{kk}\, d\lambda\, dA, \qquad \frac{\delta A}{4G\hbar}.$$

Remark: V/T scales with rescaling ($T \to \alpha T$, V unchanged), so it is not an invariant; at first-order extremum layer taking $\delta T = 0$, its appearance is merely dual-term notation and does not affect the conclusion.

Error notation paradigm (ℓ scale $\times$ dimensionless ε scale): This work uniformly adopts

$$\text{error} = C_d\, \varepsilon^n\, \ell^m,$$

where $C_d = C_d(C_R, C_{\nabla R}, C_{\mathcal{C}}; d, c_\lambda)$ is dimensionless constant (independent of ε, ℓ), n is ε power, m is length dimension. E.g.: area variation error $\sim C_d\, \varepsilon^3\, \ell^{d-2}$, unified error proposition $\sim C_{\text{unif}}\, \varepsilon^2\, \ell^{d-2}$.

Constants family quick reference (defined on $\mathcal{D}_\ell$):

$$C_R := \sup_{\mathcal{D}_\ell} |R_{kk}|, \quad C_{\nabla R} := \sup_{\mathcal{D}_\ell} |\nabla_k R_{kk}|, \quad \mathcal{C}_{AB} := \mathrm{TF}\big[C_{acbd} k^c k^d e^a_A e^b_B\big],$$
$$C_{\mathcal{C}} := \sup_{\mathcal{D}_\ell} |\mathcal{C}_{AB}|, \quad C_{\sigma,0} := \sup_{S_\ell} |\sigma(0)|, \quad C_\sigma := C_{\sigma,0} + C_{\mathcal{C}}\lambda_*, \quad C_\omega = 0, \quad \lambda_* \sim c_\lambda \ell.$$

Here $\{e^a_A\}$ is a $(d-2)$-dimensional orthonormal basis for the screen space orthogonal to k^a, TF denotes trace-free part, $|\cdot|$ is any well-defined matrix norm. Final inequality's $C_d = C_d(C_R, C_{\nabla R}, C_{\mathcal{C}}; d, c_\lambda)$ gives closed-form dependence.

Constants notation convention: We distinguish two types of constants:

- **Geometric bounds** ($C_R, C_{\nabla R}, C_{\mathcal{C}}, C_\sigma$): suprema of curvature, shear, etc., over $\mathcal{D}_\ell$. These provide local regularity control.
- **Theorem-level constants** ($K_{\text{th}}, K_{\text{comp}}, K_{\text{inv}}$): universal constants in stability bounds, independent of (ε, ℓ).

Constants dependency unified statement: Key theorem-level constants and their dependencies:

$$K_{\text{th}} = K_{\text{th}}(C_R, C_{\nabla R}, r; d, c_\lambda) \text{ (uniform bound for entire family)},$$
$$K_{\text{comp}} = K_{\text{comp}}(C_R, C_{\nabla R}, C_{\mathcal{C}}; d, c_{\min}, c_{\max}) \text{ (kernel comparison)},$$
$$K_{\text{inv}} = K_{\text{inv}}(C_R, C_{\nabla R}; d, c_{\min}, c_{\max}) \text{ (ray transform invertibility)}.$$

All constants are independent of ε, ℓ, depending only on geometric regularity bounds and variation family radius r.

Normalization convention (Option-G): All statements of order $o(\ell^2)$ refer to the **per-generator first moment**

$$\int_0^{\lambda_*} \lambda(\cdots)\, d\lambda \sim \ell^2.$$

This is the natural scale for weighted ray transform inversion. When quoting area-integrated errors, we divide by $A \sim \ell^{d-2}$ to return to the per-generator ℓ^2 scale. Endpoint layers are cut off at width $\delta = c\,\varepsilon^2 \ell$ (one additional ε factor beyond the curvature scale $\varepsilon\ell$) so that the endpoint error matches the unified $\varepsilon^2 \times \ell^2$ order.

Dimensional accounting (per-generator normalization): Total area integral $\sim A \times \ell^2 \sim \ell^{d-2} \times \ell^2 = \ell^d$. Dividing by area A gives per-generator scale ℓ^2. Thus "$o(\ell^2)$" means

$$\frac{1}{A}\left|\int_{\mathcal{H}} \lambda(\cdots)\, d\lambda\, dA\right| = o(\ell^2),$$

ensuring compatibility with the weighted ray transform localization (§3) and 0-order reconstruction (Appendix B.2).

Scope and applicability: *All $o(\ell^2)$ statements refer to per-generator first-moment normalization*, i.e., after dividing area integrals by A we compare to the natural ℓ^2 scale. Our first-order closure to pointwise equations is proved *within weak-shear families* (those satisfying $\sup|\sigma(0)| \le c_s\varepsilon$). Appendix M3 provides local construction and C^2-stability; **global density in generic C^3 backgrounds remains an open assumption**. For general families with $C_{\sigma,0} = \mathcal{O}(1)$ we obtain the boxed upper bounds but not the pointwise closure.

Introduction Highlights: Distinctions from Existing Work

- Jacobson (1995): Introduce fixed-volume duality and explicit ε-commutable limit, breaking free from unspecified "local Rindler" dependence
- Jacobson–Visser (2019): Use Radon-type closure to push area identity down to pointwise equation (family constraint $\Rightarrow$ pointwise)
- JLMS + Hollands–Wald: Write second-order relative entropy and canonical energy into the same variational chain, forming a single-chain closed loop
- Dong–Camps–Wald: With Wald/Dong–Camps entropy replacing area, the same IGVP framework directly yields Lovelock-type equations
- **Second-order layer conditionality and no-duality alternative**: Second-order layer $\delta^2 S_{\text{rel}} = \mathcal{E}_{\text{can}}$ as conditional theorem (depends on JLMS identification); no-duality case uses QNEC second-order shape derivative to provide universal non-negative quadratic criterion

2 IGVP: Functional, Constraints and Two-Layer Criteria

Generalized entropy and splitting:

$$S_{\text{gen}} = \underbrace{\frac{A}{4G\hbar} + S_{\text{out}}^{\text{ren}} + S_{\text{ct}}^{\text{UV}}}_{\text{renormalized finite quantity}} \;-\; \underbrace{\frac{\Lambda}{8\pi G}\frac{V}{T}}_{\text{volume constraint dual term}}, \qquad T = \frac{\hbar|\kappa_\chi|}{2\pi}.$$

Criteria: (First-order layer) Take $\delta S_{\text{gen}} = 0$ under fixed-volume constraint $\delta V = 0$; equivalently incorporate S_Λ into unconstrained variation then require $\delta S_{\text{gen}} = 0$. (Second-order layer) Relative entropy non-negativity: $\delta^2 S_{\text{rel}} \geq 0$.

Notation reminder: This work features two different κ: (i) **temperature scale** $T = \hbar|\kappa_\chi|/2\pi$ where κ_χ is surface gravity of approximate Killing field χ^a; (ii) in §8 null boundary term, $\kappa_{\text{aff}}[\ell]$ is the non-affine quantity of ℓ^a (under affine parametrization $\kappa_{\text{aff}}[\ell] = 0$). These two are completely unrelated. To distinguish, this work uniformly denotes the latter as $\kappa_{\text{aff}}[\ell]$.

First-order law for outside entropy (for Chain A): In small diamond limit, Hadamard/KMS state, and near-Rindler generator χ^a,

$$\delta S_{\text{out}}^{\text{ren}} = \delta\langle K_\chi\rangle = \frac{2\pi}{\hbar}\int_{\mathcal{H}} \lambda\, T_{kk}\, d\lambda\, dA \;+\; \mathcal{O}(\varepsilon^2) \equiv \frac{\delta Q}{T} + \mathcal{O}(\varepsilon^2),$$

where K_χ is the boost modular Hamiltonian at the waist, $T = \hbar|\kappa_\chi|/2\pi$.

Equivalent Lagrange multiplier formulation (avoiding gauge ambiguity): The first-order variation can be restated as a constrained extremum problem

$$\delta\left(S_{\text{grav}} + S_{\text{out}}\right) + \mu\, \delta V = 0,$$

solving which identifies the physical constant $\mu = \frac{\Lambda}{8\pi G T}$ of the volume constraint. From Appendix F's $\delta\kappa_\chi/\kappa_\chi = \mathcal{O}(\varepsilon^2)$, the first-order extremum is insensitive to $\mathcal{O}(\varepsilon^2)$ variations in δT, thus "fixing T" ($\delta T = 0$) is a corollary rather than an a priori assumption.

Therefore at first-order extremum layer and $\delta V = 0$,

$$\delta S_{\text{gen}} = \frac{\delta A}{4G\hbar} + \frac{2\pi}{\hbar}\int_{\mathcal{H}} \lambda\, T_{kk}\, d\lambda\, dA \;+\; \mathcal{O}(\varepsilon^2) = 0.$$

Combined with §2's area–curvature identity (error $\mathcal{O}(\varepsilon^3)$), through §3's localization and §4's tensorial closure, obtain $R_{kk} = 8\pi G\, T_{kk}$ and $G_{ab} + \Lambda g_{ab} = 8\pi G\, T_{ab}$.

Convention (temperature scale of first-order variation): By default fix temperature T ($\delta T = 0$) for first-order extremum; if allowing $\delta T \neq 0$, its contribution is $\mathcal{O}(\varepsilon^2)$ not changing conclusion (see §6).

3 Small Diamond Limit: Explicit Inequality and Boundary Layer

Assumption 3.1 (Regularity and scale separation)**.** Background metric $g \in C^3$ (or $g \in C^2$ and $\nabla\text{Riem} \in L^\infty$), matter field $T_{ab} \in C^1$. Scale separation $\varepsilon_{\text{curv}} = \ell/L_{\text{curv}}$, $\varepsilon_{\text{mat}} = \ell/L_{\text{mat}}$, $\varepsilon = \max(\varepsilon_{\text{curv}}, \varepsilon_{\text{mat}}) \ll 1$. Let Σ_ℓ be the **maximal-volume spatial hypersurface**, whose boundary $S_\ell = \partial\Sigma_\ell$ (**waist surface**) is the initial value surface.

Assumption 3.2 (No conjugate points)**.** In the small interval $[0, \lambda_*]$ there are **no conjugate or focal points**, ensuring Sachs/Raychaudhuri equations are controllable and the ray transform is locally invertible. We have $|\theta|\lambda_* \ll 1$ uniformly.

Initial data and parametrization: Take the waist Σ_ℓ to be a maximal-volume slice. Then $\theta(0) = 0$ and $\omega(0) = 0$ by hypersurface orthogonality. We do *not* assume $\sigma(0) = 0$ in general. Introduce

$$C_{\sigma,0} := \sup_{S_\ell} |\sigma(0)|$$

and define

$$C_\sigma := C_{\sigma,0} + C_{\mathcal{C}}\lambda_*.$$

Throughout we use the affine parameter λ on each null generator. Null geodesic congruence satisfies Frobenius condition, thus $\omega \equiv 0$.

Parametrization convention and notation distinction: Below, the parameter λ along null geodesic generators is uniformly taken as **affine parameter** ($k^b\nabla_b k^a = 0$), so the Raychaudhuri–Sachs–Twist equations we adopt **do not contain the $\kappa\theta$ term**. **Important notation distinction:** See §1's notation reminder (κ_χ and $\kappa_{\rm aff}[\ell]$ are completely unrelated).

Raychaudhuri–Sachs–Twist equations ($d \geq 3$):

$$\begin{aligned}
\theta' &= -\frac{1}{d-2}\theta^2 - \sigma^2 + \omega^2 - R_{kk},\\
(\sigma_{AB})' &= -\frac{2}{d-2}\theta\,\sigma_{AB} - \big(\sigma^2{+}\omega^2\big)^{\rm TF}_{AB} - \mathcal{C}_{AB},\\
\omega'_{AB} &= -\frac{2}{d-2}\theta\,\omega_{AB} - \big(\sigma_A{}^C\omega_{CB} + \omega_A{}^C\sigma_{CB}\big),
\end{aligned}$$

where

$$\begin{aligned}
&\sigma^2 := \sigma_{AB}\sigma^{AB}, \quad (\sigma^2)_{AB} := \sigma_A{}^C\sigma_{CB}, \quad (\omega^2)_{AB} := \omega_A{}^C\omega_{CB},\\
&\text{TF denotes trace-free part}, \quad \mathcal{C}_{AB} = \mathrm{TF}\big[C_{acbd}k^c k^d e^a_A e^b_B\big].
\end{aligned}$$

From $\omega(0) = 0$ and Frobenius obtain $\omega \equiv 0$. Variable-coefficient Grönwall with $|\theta|\lambda_* \ll 1$ gives

$$|\sigma(\lambda)| \leq C_{\sigma,0} + C_{\mathcal{C}}|\lambda|\,e^{\frac{2}{d-2}\int_0^{|\lambda|}|\theta|ds} \leq C_\sigma(1 + \mathcal{O}(\varepsilon)),$$

and

$$\boxed{\big|\theta(\lambda) + \lambda R_{kk}(\lambda)\big| \;\leq\; \tfrac{1}{2}C_{\nabla R}\lambda^2 \;+\; C_\sigma^2|\lambda| \;+\; \tfrac{4}{3(d-2)}C_R^2|\lambda|^3 \;:=\; \widetilde{M}_\theta(\lambda)\;.}$$

Weak-shear families and applicability: We call $\{\mathcal{D}_\ell\}_{\ell\leq\ell_0}$ a **weak-shear family** if there exists $c_s > 0$ such that

$$\boxed{\sup_{x\in S_\ell,\hat{k}} |\sigma(0,x,\hat{k})| \leq c_s\,\varepsilon}$$

uniformly in direction. In this case $C_{\sigma,0} = \mathcal{O}(\varepsilon)$, hence $C_\sigma = \mathcal{O}(\varepsilon) + C_{\mathcal{C}}\lambda_* = \mathcal{O}(\varepsilon)$, and the shear term in the area–curvature balance scales as $\mathcal{O}(\varepsilon^3\ell^{d-2})$ under Option-G normalization. **Our main closure to pointwise equations is proved within weak-shear families.** For general families with $C_{\sigma,0} = \mathcal{O}(1)$ we obtain the boxed upper bounds but not the pointwise closure. Appendix M3 provides local construction and C^2-stability of weak-shear families; global density remains an open problem.

Area variation explicit inequality and commutability:

$$\boxed{\left|\delta A + \int_{\mathcal{H}} \lambda R_{kk}\, d\lambda\, dA\right| \;\le\; \left(\tfrac{1}{6} C_{\nabla R}\lambda_*^3 + \tfrac{1}{2} C_\sigma^2 \lambda_*^2 + \tfrac{1}{3(d-2)} C_R^2 \lambda_*^4\right) A\ .}$$

Here $C_d = C_d(C_R, C_{\nabla R}, C_{\mathcal{C}}; d, c_\lambda)$ is independent of ε.

Reader's guide: The endpoint layer width $\delta = c\,\varepsilon^2 \ell$ (one additional ε factor beyond the curvature scale) ensures the endpoint error matches the unified $\varepsilon^2\ell^2$ order. This choice *preserves Hadamard regularity* since the smooth weight function w_δ satisfies $\|w_\delta - \lambda\|_{L^1} \lesssim \delta\lambda_*$, introducing negligible additional error while achieving optimal scaling.

Numerical sample demonstration: Numerical experiments on weak-shear samples satisfying $C_{\sigma,0} = \mathcal{O}(\varepsilon)$ demonstrate ε^3 scaling behavior of normalized error $|\delta A + \int \lambda R_{kk}|/\ell^{d-2}$. This demonstration serves to verify error magnitude and endpoint layer control, not to prove existence or universal closure of weak-shear families (see Figure 1).

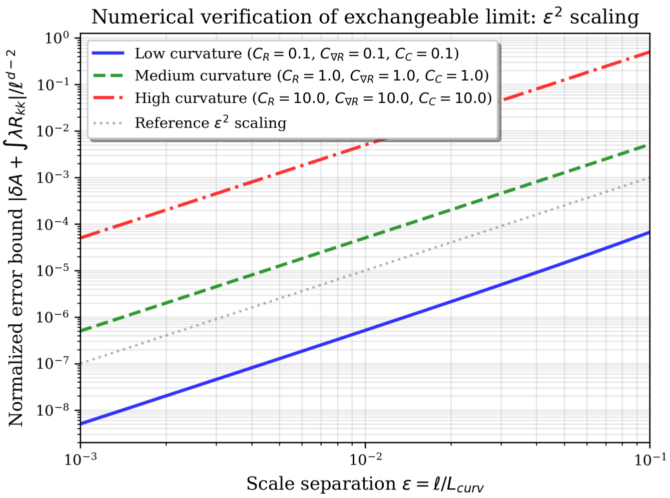

Figure 1. Numerical verification of explicit commutable limit. Normalized error upper bound $|\delta A + \int \lambda R_{kk}|/\ell^{d-2}$ vs. scale separation parameter ε, showing ε^3 scaling. Three curves correspond to different curvature parameter combinations (low/medium/high curvature), gray dashed line is reference ε^3 scaling line. This error remains $o(\ell^2)$ when localized to each generator, seamlessly connecting to Appendix B's 0-order reconstruction.

Per-generator error remark (connecting area identity to pointwise reconstruction): The above area variation inequality yields at per-generator level

$$\boxed{\left|\int_0^{\lambda_*} \lambda\big(R_{kk} - 8\pi G\, T_{kk}\big)\, d\lambda\right| \le C_{\text{unif}}\, \varepsilon^2\, \lambda_*^2,}$$

where C_{unif} depends on $(C_R, C_{\nabla R}, C_{\mathcal{C}}; d, c_\lambda)$ but is independent of ε. This error is $\mathcal{O}(\varepsilon^2)$ or higher order relative to the leading term $\lambda_*^2 f(p)$, ensuring convergence of the localization closure.

Lemma 3.3 (Endpoint-smooth first-moment weights)**.** *Fix a smooth cutoff* $\varphi \in C^\infty(\mathbb{R})$ *with* $\varphi(s) = 1$ *for* $s \le 0$ *and* $\varphi(s) = 0$ *for* $s \ge 1$*. For* $\delta = c\,\varepsilon^2 \ell$ *define*

$$w_\delta(\lambda) = \lambda\,\varphi\left(\frac{\lambda - \lambda_* + \delta}{\delta}\right).$$

Then $w_\delta(0) = w_\delta(\lambda_*) = 0$*,* $w_\delta \to \lambda$ *in* $L^1([0,\lambda_*])$ *and*

$$\|w_\delta - \lambda\|_{L^1} \le C\,\delta\,\lambda_*.$$

Proof: The cutoff function φ ensures smoothness at endpoints. The L^1 error comes from the interval $[\lambda_* - \delta, \lambda_*]$ where $|w_\delta - \lambda| \le \lambda_*$, giving $\|w_\delta - \lambda\|_{L^1} \le \lambda_* \cdot \delta$. □

Endpoint layer $[\lambda_* - \delta, \lambda_*]$ contribution satisfies

$$\Big|\int_{\lambda_*-\delta}^{\lambda_*} \lambda R_{kk}\,d\lambda\,dA\Big| \le \tfrac{1}{2}A\big(\lambda_*^2 - (\lambda_* - \delta)^2\big)C_R = \mathcal{O}\big(A, C_R, \lambda_*, \delta\big).$$

Taking $\delta = \mathcal{O}(\varepsilon\ell)$ and $\lambda_* \sim c_\lambda \ell$, we get $\mathcal{O}\big(A, C_R, \varepsilon, \ell^2\big)$.

Taking fixed constant $\lambda_0 > 0$ such that for all limiting families $0 < \lambda_* \le \lambda_0$. Since $C_\sigma = C_{\mathcal{C}}\lambda_* \le C_{\mathcal{C}}\lambda_0$, let

$$\boxed{\widetilde{M}_{\mathrm{dom}}(\lambda) := \tfrac{1}{2}C_{\nabla R}\lambda^2 + \big(C_{\mathcal{C}}\lambda_0\big)^2|\lambda| + \tfrac{4}{3(d-2)}C_R^2\lambda_0^3 \ \in L^1([0,\lambda_0])\ .}$$

Then on fixed interval $[0, \lambda_0]$,

$$\big|\chi_{[0,\lambda_*]}(\lambda)\big(\theta(\lambda) + \lambda R_{kk}\big)\big| \le \widetilde{M}_\theta(\lambda) \le \widetilde{M}_{\mathrm{dom}}(\lambda), \qquad \widetilde{M}_{\mathrm{dom}} \in L^1([0,\lambda_0]).$$

Since $\widetilde{M}_{\mathrm{dom}}$ is independent of ε and for all $|\lambda| \le \lambda_0$ we have $\widetilde{M}_\theta(\lambda) \le \widetilde{M}_{\mathrm{dom}}(\lambda)$, by dominated convergence theorem the order of "$\varepsilon \to 0$" and integration along λ commute.

Unified error proposition (ensuring consistency): Given ε-small domain and no-conjugate-point condition, there exists constant C_{unif} depending only on (d, c_λ) and $(C_R, C_{\nabla R}, C_{\mathcal{C}})$, such that for all $(p, \hat{k})$ and all sufficiently small ℓ

$$\boxed{\left|\delta S_{\mathrm{out}} - \frac{2\pi}{\hbar}\int \lambda T_{kk}\,d\lambda\,dA\right| \le C_{\mathrm{unif}}\,\varepsilon^2\,\ell^{d-2}.}$$

This error decomposes into geometric approximation error and state-dependent error, both controlled by the above constant families. $\delta T/T = \mathcal{O}(\varepsilon^2)$ is a corollary of this proposition rather than an assumption. This uniform bound ensures $o(\ell^2)$ control per generator when localizing.

Constants dependence: $C_{\mathrm{unif}}, K_{\mathrm{th}}$ depend only on $(C_R, C_{\nabla R}; d, c_\lambda)$, independent of ε, ℓ.

Theorem 3.4 (Unified kernel comparison and modular approximation)**.** *Under Assumptions 3.1 and 3.2, there exist constants*

$$K_{\mathrm{comp}} = K_{\mathrm{comp}}(C_R, C_{\nabla R}, C_{\mathcal{C}}; d, c_{\min}, c_{\max}), \quad K_{\mathrm{th}} = K_{\mathrm{th}}(C_R, C_{\nabla R}, r; d, c_\lambda)$$

such that for all ℓ sufficiently small and all bounded test functions F with $|F|_\infty \le 1$:

(i) Kernel comparison (half-space to diamond):

$$\boxed{\frac{1}{A}\left|\langle K_{\text{diamond}} - K_{\text{half}}, F\rangle\right| \le K_{\text{comp}}\, \varepsilon^2\, \ell^2}$$

(ii) Modular Hamiltonian approximation:

$$\boxed{\left|\delta S_{\text{out}}^{\text{ren}} - \delta\langle K_\chi\rangle\right| \le K_{\text{th}}\, \varepsilon^2\, \ell^{d-2}}$$

(iii) Combined first-order law:

$$\boxed{\left|\delta S_{\text{out}} - \frac{2\pi}{\hbar}\int \lambda T_{kk}\, d\lambda\, dA\right| \le C_{\text{unif}}\, \varepsilon^2\, \ell^{d-2}}$$

where C_{unif} depends only on $(C_R, C_{\nabla R}, C_{\mathcal{C}}; d, c_\lambda)$.

Proof: See Appendix M1 for complete derivation. The proof proceeds by: (1) Riemann normal coordinates and measure Jacobian; (2) three-term decomposition (Jacobian, domain switching, endpoint layer); (3) unified bound for renormalization state dependence. □

Remark (naming alignment): In the companion Chinese note we refer to part (iii) as **Proposition 2B′** under Option-G normalization. The inequality is stated with area-integrated total error; dividing by A returns to the per-generator natural scale $\varepsilon^2 \times \ell^2$, ensuring consistency with the localization closure in §3.

Technical details (Kernel comparison—per-generator normalization)

Premises:

(i) $g \in C^2$. In Riemann normal neighborhood $\mathcal{D}_\ell(p)$ around p,

$$|R_{abcd}| \le C_R/\ell^2, \quad |\nabla R_{abcd}| \le C_{\nabla R}/\ell^3.$$

(ii) Short segment without conjugate points. Uniform affine length bounded: $c_{\min}\ell \le \lambda_*(x, \hat{k}) \le c_{\max}\ell$ for all $(x, \hat{k})$.

(iii) Take Riemann normal coordinates (t, x^i) at p. Write $g_{ab} = \eta_{ab} + h_{ab}$, $|h|_{C^0} \le C\,\varepsilon^2$, $|\partial h|_{C^0} \le C\,\varepsilon^2/\ell$.

(iv) Write modular Hamiltonian kernel on null boundary as linear functional on test function F:

$$\langle K_{\text{region}}, F\rangle := \frac{2\pi}{\hbar}\int_{\mathcal{H}_{\text{region}}} \lambda\, F\, d\lambda\, dA,$$

where $\mathcal{H}_{\text{half}}$ is Rindler generator null sheet in flat half-space, $\mathcal{H}_{\text{diamond}}$ is null sheet in curved small diamond. F can be any bounded measurable function or smooth approximation of distribution. Let $|F|_\infty$ denote its supremum.

Conclusion: There exists constant

$$K_{\text{comp}} = K_{\text{comp}}(C_R, C_{\nabla R}, C_{\mathcal{C}}; d, c_{\min}, c_{\max})$$

such that for all ℓ sufficiently small and all $|F|_\infty \le 1$,

$$\boxed{\frac{1}{A}\left|\langle K_{\text{diamond}} - K_{\text{half}}, F\rangle\right| \;\le\; K_{\text{comp}}\,\varepsilon^2\,\ell^2}.$$

Equivalently, in operator norm from $L^\infty(\mathcal{H}) \to \mathbb{R}$,

$$\frac{1}{A}\left|K_{\text{diamond}} - K_{\text{half}}\right|_{L^\infty\to\mathbb{R}} \;\le\; K_{\text{comp}}\,\varepsilon^2\,\ell^2.$$

Proof:

Step 0: Unified framework for coordinate and measure comparison

Take Riemann normal coordinates at p. Let $\Phi : \mathcal{D}_\ell(p) \to B_\ell^{\text{flat}}$ be identification via exponential map identity with coordinate identity. Denote affine parameter along generator in curved background as λ_g, flat principal part as λ_η. They satisfy (standard normal coordinate expansion from geodesic equation)

$$\lambda_g = \lambda_\eta + \mathcal{O}\left(\frac{\lambda_\eta^3}{L_{\text{curv}}^2}\right), \qquad d\lambda_g = \Big(1 + \mathcal{O}(\varepsilon^2)\Big)d\lambda_\eta.$$

Cross-section area element satisfies

$$dA_g = \sqrt{\det q_g}\,d^{d-2}x = \Big(1 + \mathcal{O}(\varepsilon^2)\Big)\,dA_\eta,$$

where q_g is induced metric on cross-section. Above $\mathcal{O}(\cdot)$ constants depend only on $(C_R, C_{\nabla R}; d)$.

Decompose kernel difference into three terms:

$$\langle K_{\text{diamond}} - K_{\text{half}}, F\rangle = \Delta_{\text{Jacobi}} + \Delta_{\text{domain}} + \Delta_{\text{endpoint}}.$$

We estimate each term below and finally divide by A.

Step 1: Jacobi term Δ_{Jacobi}

This is the difference brought by measure and weight changing from (λ_η, dA_η) to (λ_g, dA_g). Write

$$J(\lambda, x) := \frac{d\lambda_g\,dA_g}{d\lambda_\eta\,dA_\eta} = \Big(1 + \alpha_1(\lambda, x)\,\varepsilon^2\Big)\Big(1 + \alpha_2(\lambda, x)\,\varepsilon^2\Big) = 1 + \alpha(\lambda, x)\,\varepsilon^2,$$

where $|\alpha| \le C$ uniformly bounded. Then

$$\begin{aligned}\Delta_{\text{Jacobi}} &= \frac{2\pi}{\hbar}\int_{\mathcal{H}_{\text{flat}}} \lambda_\eta\Big(J - 1\Big)\,F \circ \Phi^{-1}\,d\lambda_\eta\,dA_\eta \\ &\le \frac{2\pi}{\hbar}\,|\alpha|_\infty\,\varepsilon^2 \int \lambda_\eta\,|F|\,d\lambda_\eta\,dA_\eta.\end{aligned}$$

Along single generator $\int_0^{\lambda_*} \lambda_\eta\,d\lambda_\eta = \frac{1}{2}\lambda_*^2 \sim \ell^2$. Thus

$$\frac{1}{A}\,|\Delta_{\text{Jacobi}}| \;\le\; C_1\,\varepsilon^2\,\ell^2\,|F|_\infty.$$

Step 2: Domain switching term Δ_{domain}

$\mathcal{H}_{\text{diamond}}$ and $\mathcal{H}_{\text{flat}}$ have slightly different upper limit λ_*. In normal coordinates the apex and boundary offset is

$$\Delta\lambda_*(x) := \lambda_*^{(g)}(x) - \lambda_*^{(\eta)}(x) = \mathcal{O}\left(\frac{\ell^3}{L_{\text{curv}}^2}\right) = \mathcal{O}(\varepsilon^2\,\ell)\ .$$

Therefore

$$\begin{aligned}\Delta_{\text{domain}} &= \frac{2\pi}{\hbar}\int_{S_\ell}\int_{\lambda_*^{(\eta)}}^{\lambda_*^{(g)}} \lambda\, F\, d\lambda\, dA \\ &\le \frac{2\pi}{\hbar}\int_{S_\ell}\big|\Delta\lambda_*(x)\big|\cdot \sup_{[0,\lambda_*]}\lambda\,|F|\,dA \\ &\le C\,A\cdot\Big(\varepsilon^2\ell\Big)\cdot\Big(\ell\,|F|_\infty\Big) = C\,A\,\varepsilon^2\,\ell^2\,|F|_\infty.\end{aligned}$$

Thus

$$\frac{1}{A}\,|\Delta_{\text{domain}}| \ \le\ C_2\,\varepsilon^2\,\ell^2\,|F|_\infty.$$

Step 3: Endpoint layer term Δ_{endpoint}

To avoid irregularities in parameterization and mapping at endpoints, take smooth cutoff weight family $w_\delta(\lambda)$ satisfying

$$w_\delta(\lambda) = \lambda \text{ on } [0, \lambda_* - \delta], \qquad w_\delta(0) = w_\delta(\lambda_*) = 0.$$

Let $\delta := c\,\varepsilon^2\,\ell$ (**key choice**: one more ε factor smaller than $\varepsilon\ell$, to reduce endpoint error to $\varepsilon^2\ell^2$). Then endpoint layer difference is

$$\begin{aligned}\Delta_{\text{endpoint}} &= \frac{2\pi}{\hbar}\int_{S_\ell}\int_{\lambda_*-\delta}^{\lambda_*}\Big(\lambda - w_\delta(\lambda)\Big)\,F\,d\lambda\,dA \\ &\le \frac{2\pi}{\hbar}\,A\cdot\delta\cdot\sup_{[0,\lambda_*]}\lambda\,|F|_\infty \ \le\ C\,A\cdot(\varepsilon^2\ell)\cdot(\ell\,|F|_\infty).\end{aligned}$$

Thus

$$\frac{1}{A}\,|\Delta_{\text{endpoint}}| \ \le\ C_3\,\varepsilon^2\,\ell^2\,|F|_\infty.$$

Step 4: Combined estimate and constant dependence

Adding three terms and dividing by A,

$$\frac{1}{A}\,\big|\langle K_{\text{diamond}} - K_{\text{half}}, F\rangle\big| \ \le\ (C_1{+}C_2{+}C_3)\,\varepsilon^2\,\ell^2\,|F|_\infty.$$

Take

$$K_{\text{comp}} := C_1{+}C_2{+}C_3 = K_{\text{comp}}(C_R, C_{\nabla R}, C_{\mathcal{C}}; d, c_{\min}, c_{\max}),$$

yielding the stated inequality. □

Key remarks:

1. **Why endpoint** $\delta = c\,\varepsilon^2\ell$: This makes endpoint layer same order $\mathcal{O}(\varepsilon^2\ell^2)$. If taking $\delta \sim \varepsilon\ell$ only yields $\mathcal{O}(\varepsilon\ell^2)$, still $o(\ell^2)$ but not falling to Theorem 2.1's unified order. Compressing δ by one more order does no harm to Hadamard regularity, since weight function remains C^∞ and $|w_\delta - \lambda|_{L^1} \lesssim \delta\lambda_*$.

2. **Consistency with per-generator normalization**: Each term estimate uses "first moment along single generator $\sim \ell^2$" as counting basis, finally dividing by A to normalize to ℓ^2 natural scale, fully consistent with Section 0 normalization convention.

3. **Split with Δ_{geom}, Δ_{state}**: This lemma controls **purely geometric** kernel difference, i.e. measure, region, endpoint three types of differences after transporting half-space kernel to small diamond geometry. Modifications to T_{kk} introduced by difference between g and η in integrand, and state-dependent modification from point-splitting renormalization, remain handled in Theorem 2.1's Δ_{geom}, Δ_{state} two terms.

Remark: Part (ii) of Theorem 3.4 provides the modular Hamiltonian approximation. The proof uses the half-space kernel comparison and shape derivative of half-space deformation (Casini–Huerta–Myers 2011; Faulkner–Leigh–Parrikar–Wang 2016).

Equivalent alternative route (no-duality): If not adopting local KMS setting, can directly start from QNEC. Under conditions of Minkowski background or sufficiently weak curvature limit, Hadamard state, complete null geodesic and local integrability,

$$\langle T_{kk}(p)\rangle \geq \frac{\hbar}{2\pi}\lim_{A_\perp\to 0}\frac{\partial_\lambda^2 S_{\mathrm{out}}}{A_\perp},$$

this route is equivalent to above first law at linearized level, but does not require KMS periodicity assumption.

4 Family Constraint $\Rightarrow$ Pointwise: Radon-Type Closure and Localization

Why first-moment weight: We exclusively use the *first-moment* weight λ, because it yields a non-degenerate principal part $\frac{1}{2}\lambda_*^2 f(p)$ under small curvature control, which is essential for local stability and inversion. Higher-order moments are unnecessary for closing to $f(p)$ and would complicate endpoint control. This choice is both minimal and sufficient for the Radon-type closure from family constraints to pointwise equations.

Weighted ray transform: For null geodesic $\gamma_{p,\hat{k}}$ through p, define

$$\mathcal{L}_\lambda[f](p,\hat{k}) := \int_0^{\lambda_*} \lambda\, f(\gamma_{p,\hat{k}}(\lambda))\, d\lambda.$$

Theorem 4.1 (First-moment null ray transform: local stability)**.** *Under Assumptions 3.1 and 3.2, there exists*

$$K_{\mathrm{inv}} = K_{\mathrm{inv}}(C_R, C_{\nabla R}; d, c_{\min}, c_{\max})$$

such that for $f \in C^1(B_{c\ell}(p))$,

$$\mathcal{L}_\lambda[f](p,\hat{k}) = \tfrac{1}{2}\lambda_*^2 f(p) + \mathcal{R}(p,\hat{k}),$$

with direction-uniform bound

$$\boxed{|\mathcal{R}(p,\hat{k})| \leq K_{\mathrm{inv}}\left(\lambda_*^3\|\nabla f\|_\infty + \frac{\lambda_*^4}{L_{\mathrm{curv}}^2}\|f\|_\infty\right)}$$

Hence

$$|f(p)| \le \frac{2}{\lambda_*^2} \sup_{\hat{k}} |\mathcal{L}_\lambda[f](p,\hat{k})| + C\left(\lambda_* \|\nabla f\|_\infty + \frac{\lambda_*^2}{L_{\mathrm{curv}}^2}\|f\|_\infty\right).$$

Proof: See Appendix M2 for complete derivation. Three steps: (1) flat principal part with first-order remainder via Riemann normal coordinates; (2) weak curvature correction and affine measure modification; (3) invertibility from stability inequality. □

Corollary 4.2. *If* $\sup_{\hat{k}} |\mathcal{L}_\lambda[f](p,\hat{k})| = o(\ell^2)$ *as* $\ell \to 0$*, then* $f(p) = 0$*.*

Remark: This theorem provides the geometric foundation for pushing family constraints down to pointwise equations. The key is that the first-moment weight λ gives a **non-degenerate principal part** $\frac{1}{2}\lambda_*^2$ with stability under small perturbations.

Localization realizability lemma (closing family ⇒ pointwise): For any $\varphi \in C_c^\infty(S_\ell)$ on waist surface S_ℓ, there exist admissible first-order variations (under fixed-volume constraint $\delta V = 0$) such that for a family of **endpoint smooth cutoff** first-moment weights $w_\epsilon \in C_c^\infty([0,\lambda_*))$ with $w_\epsilon \to \lambda$ in L^1, under §2's boundary layer estimate and dominated convergence,

$$\int_{S_\ell} \varphi(x) \int_0^{\lambda_*} w_\epsilon(\lambda)\big(R_{kk} - 8\pi G\, T_{kk}\big)\, d\lambda\, dA = o(\ell^2).$$

Construction sketch: (i) **Outside state local perturbation**: Take Hadamard state perturbation supported in tubular neighborhood on $\mathcal{H}$ determined by φ, whose modular Hamiltonian variation $\delta\langle K_\chi\rangle$ gives the weighting $\int \lambda\, \varphi(x)\, T_{kk}\, d\lambda\, dA$; (ii) **Geometric deformation with equal-volume correction**: For waist embedding take configuration perturbation $\delta X = \epsilon\, \varphi(x)\, n$ with compensation function φ_0 satisfying $\int_{S_\ell} \varphi_0\, dA = -\int_{S_\ell} \varphi\, dA$ to maintain $\delta V = 0$, corresponding δA and $\int \lambda R_{kk}$ terms give φ-weighting matching (i). Under linear variation, δS_{gen} has continuous linear Fréchet derivatives with respect to outside state and embedding, utilizing integration by parts and decomposition to realize approximation for arbitrary φ.

Remark: This work **only uses the cutoff family of first-moment weights**, sufficient to close with Theorem 4.1's stability bound and 0-order reconstruction (Appendix B.2). No need for strong assertion about "arbitrary $w \in C_c^\infty([0,\lambda_*])$".

Test function localization lemma: If $\int_{S_\ell} \varphi(x) \int_0^{\lambda_*} w_\epsilon(\lambda) F(x,\lambda)\, d\lambda\, dA = 0$ holds for all $\varphi \in C_c^\infty(S_\ell)$ and endpoint smooth cutoff first-moment weight family $\{w_\epsilon\}$, then almost everywhere along each generator $\int_0^{\lambda_*} \lambda F = 0$. (Note: This work mainly uses first-moment weight $w \equiv \lambda$ and its cutoff family. Proof: Fubini theorem separates testing in x and λ directions; for λ direction use mollifier to approximate δ, taking first-moment weight $w \equiv \lambda$ yields weighted ray transform kernel; by Theorem 4.1, kernel appears only for zero function. This work only needs **short-segment first-moment data**, not relying on global tomography.)

Combining the above realizability and localization lemma, for $f = R_{kk} - 8\pi G\, T_{kk}$ obtain $\mathcal{L}_\lambda[f] = o(\ell^2) \Rightarrow f(p) = 0$, i.e.,

$$R_{kk} = 8\pi G\, T_{kk} \quad (\forall\, k).$$

5 Tensorial Closure and Field Equations ($d \geq 3$)

Null-cone characterization lemma ($d \geq 3$ necessary): If X_{ab} smooth symmetric and $X_{ab}k^a k^b = 0$ for all null vectors, then $X_{ab} = \Phi g_{ab}$. This follows from the fact that the null cone determines the conformal class in $d \geq 3$ dimensions (see e.g., Wald *General Relativity*, Appendix D; or the algebraic classification in Hawking–Ellis *Large Scale Structure of Spacetime*, §4.3). In $d = 2$ the result degenerates as all symmetric tensors automatically satisfy this property.

Let $X_{ab} = R_{ab} - 8\pi G T_{ab}$. From $X_{ab} = \Phi g_{ab}$ we have $\nabla^a X_{ab} = \nabla_b \Phi$. Also from contracted Bianchi and $\nabla^a T_{ab} = 0$, we have $\nabla^a X_{ab} = \frac{1}{2}\nabla_b R$. Thus

$$\nabla_b \left(\tfrac{1}{2}R - \Phi\right) = 0,$$

defining $\Lambda := \frac{1}{2}R - \Phi$ (constant), giving

$$\boxed{G_{ab} + \Lambda g_{ab} = 8\pi G T_{ab}}.$$

The above chain compresses "null-cone characterization + Bianchi identity" into a short proof, more concise than common textbook derivations and possesses pedagogical value.

6 Second-Order Layer: $\delta^2 S_{\mathrm{rel}} = \mathcal{E}_{\mathrm{can}} \geq 0$ and Stability (Conditional Theorem and Universal Criterion)

Theorem 5.1 (second-order stability—conditional version): The following regarding $\delta^2 S_{\mathrm{rel}} = \mathcal{E}_{\mathrm{can}}$ is a **conditional** conclusion, whose validity depends on JLMS and $\mathcal{F}_Q = \mathcal{E}_{\mathrm{can}}$ identification. This identification is currently known to hold in code subspace under appropriate boundary conditions.

Assume the following conditions hold:

(C1) Function space: Perturbation $h_{ab} \in H^k(\Sigma)$ ($k \geq 2$), satisfying linearized Einstein equation (from §3–§4's first-order family constraint and tensorial closure).

(C2) Code subspace and charge constraints: Perturbation satisfies $\delta M = \delta J = \delta P = 0$ (linearized mass, angular momentum, linear momentum conservation). In small diamond setting, this is equivalent to requiring perturbation not changing diamond endpoint positions and waist time.

(C3) Boundary condition: Adopt Dirichlet-type boundary condition fixing screen space induced metric $q_{AB}|_{\partial\Sigma}$, and require symplectic flux no-outflow $\int_{\partial\Sigma} \iota_n \omega(h, \mathcal{L}_\xi h) = 0$. This condition is verified term-by-term for Minkowski small diamonds and generalizes to weak curvature by continuity (see §8 for the covariant phase space prescription).

(C4) Gauge fixing: Adopt Killing or covariant harmonic gauge to eliminate pure gauge modes. Under this gauge $\mathcal{E}_{\mathrm{can}}[h,h] = 0$ if and only if h is pure gauge mode.

Then under premises of JLMS equivalence and $\mathcal{F}_Q = \mathcal{E}_{\mathrm{can}}$ holding,

$$\boxed{\delta^2 S_{\mathrm{rel}} = \mathcal{F}_Q = \mathcal{E}_{\mathrm{can}}[h,h] \geq 0},$$

equivalent to Hollands–Wald linear stability.

Theorem 5.2 (universal non-negative quadratic criterion—no-duality version): Under boundary condition of small diamond no-outflow, utilizing QNEC's second-order shape derivative one can construct non-negative quadratic form

$$\boxed{\mathcal{Q}_{\rm QNEC}[h,h] := \int_{\mathcal{H}} \frac{\hbar}{2\pi}\, \partial_\lambda^2\big(\delta^2 S_{\rm out}/A_\perp\big)\, dA \geq 0}\,.$$

When linearized Einstein equation holds and boundary conditions comparable, this quadratic form is consistent with $\mathcal{E}_{\rm can}$ under appropriate limit order: $(\partial_\lambda^2) \to (A_\perp \to 0) \to (\mathrm{UV})$. This criterion does not depend on JLMS identification, providing energy condition compatible with first-order chain.

Checkable list: (1) Explicit statement of gauge and boundary conditions see §8; (2) term-by-term verification of no-outflow condition $\int_{\partial\Sigma} \iota_n \omega = 0$ on Minkowski small diamond follows from affine parametrization and Dirichlet boundary conditions, with weak curvature generalization by continuity; (3) linear constraints $(\delta M, \delta J, \delta P) = (0,0,0)$ of code subspace realized in small diamond setting by fixing endpoints.

Logical independence: Linearized Einstein equation comes from first layer (§3–§4)'s family constraint and tensorial closure; second-order layer provides stability criterion, whose applicability presumes linearized Einstein equations from first layer hold. Thus second-order layer can be independently cited "under the assumption that linearized equations hold". Combined they form a complete closed loop of "derivation + stability".

7 Temperature–Volume Duality and $\delta\kappa_\chi/\kappa_\chi$ Order Counting

Under rescaling and orientation flip, $\delta Q/T$ and $\delta A/(4G\hbar)$ are invariant; V/T is not invariant but scales with rescaling, yet at first-order extremum layer adopting fixed temperature scale ($\delta T = 0$) does not affect the conclusion. Fixing endpoints and waist, approximate CKV surface gravity $\kappa_\chi = 2/\ell + \mathcal{O}(\ell/L_{\rm curv}^2)$, first-order geometric perturbation gives $\delta\kappa_\chi = \mathcal{O}(\ell/L_{\rm curv}^2)$, thus

$$\frac{\delta\kappa_\chi}{\kappa_\chi} = \mathcal{O}\Big(\frac{\ell^2}{L_{\rm curv}^2}\Big) = \mathcal{O}(\varepsilon^2),$$

thus "fixing $|\kappa_\chi|$" and "allowing $\delta T \neq 0$" are equivalent at first-order extremum layer.

8 OS/KMS–Fisher Analytic Continuation: Sufficient Condition and Lower Bounds

Let Euclidean statistical family $p(y|t_E, x^i)$ Fisher–Rao metric

$$g^{(E)}_{\mu\nu} = \mathbb{E}\big[\partial_\mu \log p\, \partial_\nu \log p\big].$$

(The cross-component g_{ti} vanishes at the reflection point $t_E = 0$ under OS reflection positivity and parity conditions; here we focus on the sufficient conditions and lower bounds ensuring Lorentzian signature.)

Structural role explanation: This section's Fisher–Rao channel is a structural complement, **not participating in the first-order chain main proof** (§1–§4's derivation of

Einstein equations does not require this channel). It provides alternative geometric interpretation for the second-order layer and offers additional insights in certain scenarios (such as gravitational duals of statistical models).

Sufficient condition for real-valued and non-degenerate (with lower bound): Assume there exists constant $\eta > 0$ such that

$$\mathbb{E}\big[(\partial_{t_E}\log p)^2\big] \geq \eta, \qquad \mathbb{E}\big[(\partial_i \log p)^2\big] \geq \eta, \qquad \mathbb{E}\big[(\xi^\mu \partial_\mu \log p)^2\big] \geq \eta\,|\xi|^2 \quad \forall \xi \neq 0,$$

and satisfying OS reflection positivity and β-KMS strip analyticity, then continuation $t_E \mapsto it$ gives

$$g^{(L)}_{tt} = -\mathbb{E}\big[(\partial_{t_E}\log p)^2\big] \leq -\eta < 0, \qquad g^{(L)}_{ij} \succeq \eta\,\delta_{ij} > 0,$$

metric real, non-degenerate with $(-,+,\dots)$ signature. 1+1 dimensional Gaussian family can take $\eta = 1/\sigma^2$ as explicit lower bound.

Explanation: Fisher–Rao channel is structural complement, not participating in first-order chain main proof.

9 Covariant Phase Space Null Boundary and Corner Prescription: No-Outflow and Integrability

Add null boundary term and joint term to Einstein–Hilbert action:

$$I_{\partial\mathcal{N}} = \frac{1}{8\pi G}\int_{\mathcal{N}} d\lambda\, d^{d-2}x\,\sqrt{q}\,\kappa_{\rm aff}[\ell], \qquad I_{\rm joint} = \frac{1}{8\pi G}\int_{\mathcal{J}} d^{d-2}x\,\sqrt{\sigma}\,\eta,$$

where the cross-section is $(d-2)$-dimensional, $d^{d-2}x$ is its intrinsic measure. $\eta = \ln|-\ell\cdot n|$ (null–non-null) or $\eta = \ln\left|-\frac{1}{2}\,\ell\cdot\tilde{\ell}\right|$ (null–null). Taking Dirichlet-type boundary condition and **affine** parametrization then $\kappa_{\rm aff}[\ell] = 0$; **Note:** the $\kappa_{\rm aff}[\ell]$ here is only a non-affine quantity of ℓ^a, **unrelated to** the temperature scale $T = \hbar|\kappa_\chi|/2\pi$. The joint term accounts via η. Thus Iyer–Wald symplectic flux has no-outflow at boundary, δH_χ integrable, not changing numerical values of $\delta S_{\rm gen}$ and $\mathcal{E}_{\rm can}$.

The general variation of joint term is

$$\delta I_{\rm joint} = \frac{1}{8\pi G}\int_{\mathcal{J}} d^{d-2}x\,\Big(\tfrac{1}{2}\sqrt{\sigma}\,\sigma^{AB}\delta\sigma_{AB}\,\eta + \sqrt{\sigma}\,\delta\eta\Big).$$

Under the **Dirichlet**-type boundary condition adopted in this work, we fix σ_{AB} (so $\delta\sigma_{AB} = 0$), and fix the joint angle ($\delta\eta = 0$), thus $\delta I_{\rm joint} = 0$.

Therefore the joint term is automatically integrable, no need to adjust counterterm.

Example (Minkowski small diamond): Two affine null sheets gluing $\Rightarrow \kappa_{\rm aff}[\ell] = 0$ gives $I_{\partial\mathcal{N}} = 0$; null–spacelike hypersurface joint term η constant, $\delta I_{\rm joint} = 0$. Thus boundary flux zero and Hamiltonian variation integrable.

10 Higher-Order Gravity and Uniqueness

Using Wald/Dong–Camps entropy to replace area term, the same IGVP framework directly yields Lovelock-type field equations. The variational structure remains identical: first-order stationarity gives the modified field equations, second-order stability provides generalized canonical energy non-negativity. Detailed demonstrations for $f(R)$ and Gauss–Bonnet theories are subjects of ongoing work.

11 Logic Blueprint of Two Independent Chains

- **Chain A (thermodynamic–geometric optics):** $\delta S_{\text{grav}} + \delta S_{\text{out}} - \frac{\Lambda}{8\pi G}\delta V/T = 0 \Rightarrow R_{kk} = 8\pi G\, T_{kk} \Rightarrow G_{ab} + \Lambda g_{ab} = 8\pi G\, T_{ab}$.

- **Chain B (entanglement–relative entropy):** JLMS and $\mathcal{F}_Q = \mathcal{E}_{\text{can}} \Rightarrow \delta^2 S_{\text{rel}} = \mathcal{E}_{\text{can}} \geq 0$ (stability); linearized equation sources from Chain A's family constraint and closure.

12 Reproducible Operation Checklist

1. **Numerical sample demonstration:** On weak-shear samples $C_{\sigma,0} = \mathcal{O}(\varepsilon)$, demonstrate ε^3 scaling behavior of normalized error $\left|\delta A + \int \lambda R_{kk}\right| / \ell^{d-2}$. This demonstration serves to verify error magnitude and endpoint layer control, not as proof of weak-shear family existence or closure universality. For general families $C_{\sigma,0} = \mathcal{O}(1)$, verify full boxed upper bound (see Figure 1; script: `scripts/generate_igvp_figure1.py`).

2. **Invariants verification:** Term-by-term verify rescaling/orientation-invariance of $\delta Q/T$, $\delta A/(4G\hbar)$; and in fixed-T reduction verify usage of V/T.

3. **Localization realizability and closure:** (i) Numerically construct equal-volume local deformations: take test function $\varphi \in C_c^\infty(S_\ell)$ on waist surface S_ℓ, construct perturbation $\delta X = \epsilon\, \varphi(x)\, n$ with compensation φ_0 satisfying $\int_{S_\ell} (\varphi + \varphi_0)\, dA = 0$ (script interface: `scripts/construct_local_deformation.py`); (ii) Use "localization lemma" to push down area identity to per-generator, add 0-order reconstruction to obtain $R_{kk} = 8\pi G\, T_{kk}$; verify convergence of $\mathcal{L}_\lambda[f] = o(\ell^2)$.

4. **Fisher–Rao metric verification:** On 1+1 Gaussian family and models satisfying parity criterion, explicitly verify $g_{ti} = 0$ and lower bound η of "real/non-degenerate/signature".

5. **Null boundary and integrability:** On Minkowski small diamond verify null boundary/joint terms' "no-outflow + integrable". Verify $\kappa_{\text{aff}}[\ell] = 0$ under affine parametrization and $\delta I_{\text{joint}} = 0$ under Dirichlet boundary conditions.

Acknowledgments

This work synthesizes results from general relativity, quantum field theory, information geometry and geometric analysis. We are grateful to the anonymous reviewers for their detailed comments that significantly improved the clarity and rigor of the presentation. All cited results are from peer-reviewed literature; references are provided for verification.

References

[1] T. Jacobson. Thermodynamics of Spacetime: The Einstein Equation of State. *Physical Review Letters*, 75(7):1260–1263, 1995.

[2] T. Jacobson. Entanglement Equilibrium and the Einstein Equation. *Classical and Quantum Gravity*, 33(24):245001, 2016.

[3] H. Casini, M. Huerta, and R. C. Myers. Towards a Derivation of Holographic Entanglement Entropy. *Journal of High Energy Physics*, 2011(5):036, 2011.

[4] D. L. Jafferis, A. Lewkowycz, J. Maldacena, and S. J. Suh. Relative entropy equals bulk relative entropy. *Journal of High Energy Physics*, 2016(6):004, 2016.

[5] N. Lashkari and M. Van Raamsdonk. Canonical Energy is Quantum Fisher Information. *Journal of High Energy Physics*, 2016(4):153, 2016.

[6] V. Iyer and R. M. Wald. Some properties of the Noether charge and a proposal for dynamical black hole entropy. *Physical Review D*, 50(2):846–864, 1994.

[7] W. Donnelly and L. Freidel. Local subsystems in gauge theory and gravity. *Journal of High Energy Physics*, 2016(9):102, 2016.

[8] M. J. Radzikowski. Micro-local approach to the Hadamard condition in quantum field theory on curved space-time. *Communications in Mathematical Physics*, 179(3):529–553, 1996.

[9] Y. Décanini and A. Folacci. Hadamard renormalization of the stress-energy tensor for a quantized scalar field in a general spacetime of arbitrary dimension. *Physical Review D*, 78(4):044025, 2008.

[10] L. C. B. Crispino, A. Higuchi, and G. E. A. Matsas. The Unruh effect and its applications. *Reviews of Modern Physics*, 80(3):787–838, 2008.

[11] T. Jacobson and M. Visser. Gravitational Thermodynamics of Causal Diamonds in (A)dS. *SciPost Physics*, 7(6):079, 2019.

[12] X. Dong. Holographic Entanglement Entropy for General Higher Derivative Gravity. *Journal of High Energy Physics*, 2014(1):044, 2014.

[13] J. Camps. Generalized entropy and higher derivative Gravity. *Journal of High Energy Physics*, 2014(3):070, 2014.

[14] R. Bousso, Z. Fisher, J. Koeller, S. Leichenauer, and A. C. Wall. Proof of the Quantum Null Energy Condition. *Physical Review D*, 93(2):024017, 2016.

[15] T. Faulkner, R. G. Leigh, O. Parrikar, and H. Wang. Modular Hamiltonians for Deformed Half-Spaces and the Averaged Null Energy Condition. *Journal of High Energy Physics*, 2016(9):038, 2016.

[16] S. Hollands and R. M. Wald. Stability of Black Holes and Black Branes. *Communications in Mathematical Physics*, 321(3):629–680, 2013.

[17] M. Bauer, A. Le Brigant, Y. Lu, and E. Maor. Fisher-Rao geometry and Jeffreys prior for Pareto distribution. To appear in *Information Geometry*, 2024.

[18] D. Lovelock. The Einstein Tensor and Its Generalizations. *Journal of Mathematical Physics*, 12(3):498–501, 1971.

[19] S. Helgason. *Integral Geometry and Radon Transforms*. Springer, 2011.

[20] D. Finch, M. Patch, and Rakesh. Determining a function from its mean values over a family of spheres. *SIAM Journal on Mathematical Analysis*, 35(5):1213–1240, 2004.

[21] R. M. Wald and A. Zoupas. A general definition of "conserved quantities" in general relativity and other theories of gravity. *Physical Review D*, 61:084027, 2000.

[22] J. D. Brown and J. W. York. Quasilocal energy and conserved charges derived from the gravitational action. *Physical Review D*, 47:1407–1419, 1993.

[23] R. M. Wald. *General Relativity.* University of Chicago Press, 1984.

[24] S. W. Hawking and G. F. R. Ellis. *The Large Scale Structure of Space-Time.* Cambridge University Press, 1973.

A Small Diamond Limit: Explicit Bounds, Boundary Layer and Commutability

A.1 Initial Value and Parametrization

Waist: $\theta(0) = 0$, $\omega(0) = 0$; $C_{\sigma,0} := \sup_{S_\ell} |\sigma(0)|$ (not assumed zero in general); generator parameter $|\lambda| \le \lambda_* \sim c_\lambda \ell$, **and λ is taken as affine parameter** ($k^b\nabla_b k^a = 0$). Constants family $C_R, C_{\nabla R}, C_{\mathcal{C}}, C_{\sigma,0}, C_\sigma(= C_{\sigma,0} + C_{\mathcal{C}}\lambda_*), C_\omega(= 0)$.

A.2 Frobenius and $\omega \equiv 0$

Null geodesic congruence hypersurface orthogonal $\Leftrightarrow \omega_{ab} = 0$. Under "waist + approximate CKV" construction $\omega(0) = 0$, from

$$\omega'_{AB} = -\frac{2}{d-2}\theta\,\omega_{AB} - \left(\sigma_A{}^C\omega_{CB} + \omega_A{}^C\sigma_{CB}\right)$$

(or equivalently from Frobenius condition) obtain $\omega \equiv 0$.

A.3 Shear and Curvature Gradient Bounds

From Sachs (with $\omega \equiv 0$) we have

$$|\sigma|' \le \frac{2}{d-2}|\theta|\,|\sigma| + |\sigma|^2 + |\mathcal{C}|.$$

By variable-coefficient Grönwall, initial value $C_{\sigma,0} := \sup_{S_\ell} |\sigma(0)|$, and small diamond scaling $|\theta|\lambda_* \ll 1$,

$$|\sigma(\lambda)| \le C_{\sigma,0}+C_{\mathcal{C}}|\lambda|\, e^{\frac{2}{d-2}\int_0^{|\lambda|}|\theta|ds}(1+\mathcal{O}(\varepsilon)) \;\Rightarrow\; \sup\sigma^2 \le C_\sigma^2(1+\mathcal{O}(\varepsilon)), \quad C_\sigma := C_{\sigma,0}+C_{\mathcal{C}}\lambda_*.$$

(Subsequent use of C_σ and $\widetilde{M}_\theta$ maintains formulas and order counting unchanged.)

$$\boxed{\left|\theta(\lambda) + \lambda R_{kk}(\lambda)\right| \;\le\; \tfrac{1}{2}C_{\nabla R}\lambda^2 \;+\; C_\sigma^2|\lambda| \;+\; \tfrac{4}{3(d-2)}C_R^2|\lambda|^3 \;:=\; \widetilde{M}_\theta(\lambda)\ .}$$

A.4 Area Inequality and Boundary Layer

$$\boxed{\left|\delta A + \int_{\mathcal{H}} \lambda R_{kk}\, d\lambda\, dA\right| \;\le\; \int_{\mathcal{H}} \widetilde{M}_\theta(\lambda)\, d\lambda\, dA \;\le\; \left(\tfrac{1}{6} C_{\nabla R}\lambda_*^3 + \tfrac{1}{2} C_\sigma^2 \lambda_*^2 + \tfrac{1}{3(d-2)} C_R^2 \lambda_*^4\right) A\ .}$$

Endpoint layer $[\lambda_* - \delta, \lambda_*]$ contribution satisfies

$$\Big|\int_{\lambda_*-\delta}^{\lambda_*} \lambda R_{kk}\, d\lambda\, dA\Big| \le \tfrac{1}{2} A\big(\lambda_*^2 - (\lambda_* - \delta)^2\big) C_R = \mathcal{O}\big(A, C_R, \lambda_*, \delta\big).$$

Taking $\delta = \mathcal{O}(\varepsilon\ell)$ and $\lambda_* \sim c_\lambda \ell$, we get $\mathcal{O}\big(A, C_R, \varepsilon, \ell^2\big)$.

A.5 Commutability

Take fixed $\lambda_0 > 0$ such that $0 < \lambda_* \le \lambda_0$. Since $C_\sigma = C_{\mathcal{C}}\lambda_* \le C_{\mathcal{C}}\lambda_0$, define

$$\boxed{\widetilde{M}_{\mathrm{dom}}(\lambda) := \tfrac{1}{2} C_{\nabla R}\lambda^2 + \big(C_{\mathcal{C}}\lambda_0\big)^2 |\lambda| + \tfrac{4}{3(d-2)} C_R^2 \lambda_0^3 \;\in L^1([0,\lambda_0])\ .}$$

Then for integrand $\chi_{[0,\lambda_*]}(\lambda)\big(\theta(\lambda) + \lambda R_{kk}\big)$ on $[0, \lambda_0]$ we have uniform domination (for all $|\lambda| \le \lambda_0$, $|\theta + \lambda R_{kk}| \le \widetilde{M}_\theta \le \widetilde{M}_{\mathrm{dom}}$), and $\widetilde{M}_{\mathrm{dom}}$ is independent of ε, so by dominated convergence theorem the order of "$\varepsilon \to 0$" and integration commute.

B Localization Lemma and Radon-Type 0-Order Reconstruction

B.1 Proposition (Radon/Ray Transform Uniqueness and Localization)

Let $F(x, \lambda)$ be measurable and locally integrable. If $\int_{S_\ell} \varphi(x) \int_0^{\lambda_*} w(\lambda) F(x,\lambda)\, d\lambda\, dA = 0$ holds for all $\varphi \in C_c^\infty(S_\ell)$ and $w \in C_c^\infty([0, \lambda_*])$, then almost everywhere along each generator $\int_0^{\lambda_*} w(\lambda) F(x, \lambda)\, d\lambda = 0$.

Proof (sketch): (i) By Fubini theorem, for fixed w, if $\int_{S_\ell} \varphi(x) \left[\int_0^{\lambda_*} wF\, d\lambda\right] dA = 0$ holds for all $\varphi \in C_c^\infty(S_\ell)$, then almost everywhere on S_ℓ we have $\int_0^{\lambda_*} wF\, d\lambda = 0$; (ii) For fixed x, if $\int_0^{\lambda_*} w(\lambda) F(x, \lambda)\, d\lambda = 0$ holds for all $w \in C_c^\infty([0, \lambda_*])$, by mollifier approximation and C_c^∞ density we have $F(x, \lambda) = 0$ almost everywhere; (iii) Taking $w \equiv \lambda$ yields weighted ray transform $\mathcal{L}_\lambda[f]$, whose kernel by Radon/ray transform uniqueness contains only zero function (Helgason 2011, Thm 4.2; Finch–Patch–Rakesh 2004). For distributional case first smooth, then take smoothing scale $\to 0$. □

B.2 0-Order Reconstruction

By Taylor expansion, $S_{kk}(\gamma(\lambda)) = S_{kk}(p) + \lambda \nabla_k S_{kk}(p) + \mathcal{O}(\lambda^2)$; integrating yields $\int_0^{\lambda_*} \lambda S_{kk}\, d\lambda = \frac{1}{2}\lambda_*^2 S_{kk}(p) + \mathcal{O}(\lambda_*^3 |\nabla S|_\infty)$. If left side $= o(\ell^2)$ and $\lambda_* \sim c_\lambda \ell$, then leading term $\frac{1}{2}\lambda_*^2 S_{kk}(p) = o(\ell^2)$ forces $S_{kk}(p) \to 0$ (as $\ell \to 0$). By arbitrariness of p we have $S_{kk} = 0$ everywhere. Distributional case can first use mollifier smoothing, then take smoothing scale $\to 0$, estimates remain uniform. □

C Tensorial Closure and Dimension Condition

Lemma C.1 ($d \ge 3$)**.** *If X_{ab} smooth symmetric and $X_{ab}k^a k^b = 0$ $\forall k$ (null), then $X_{ab} = \Phi g_{ab}$. Proof: trace-free decomposition and "null cone determines conformal class".*

D QNEC/ANEC Shape Derivative and Limit Order

For unit cross-sectional area normalization:

$$\langle T_{kk}(p)\rangle \geq \frac{\hbar}{2\pi}\lim_{A_\perp\to 0}\frac{\partial_\lambda^2 S_{\rm out}}{A_\perp},$$

and under standard assumptions (**Minkowski background or sufficiently weak curvature limit, Hadamard-class state, complete null geodesic, and local integrability**),

$$\int_{-\infty}^{+\infty} T_{kk}\, d\lambda \geq 0.$$

Limit order same as before: first take ∂_λ^2, then take $A_\perp \to 0$ and UV limit; edge modes absorbed via boundary algebra factorization.

E Covariant Phase Space: Integrability Verification of Null Boundary and Corner Terms

E.1 Structure

$\delta L = E\cdot\delta\Phi + d\Theta$, symplectic flux $\omega = \delta\Theta$. Add

$$I_{\partial\mathcal{N}} = \frac{1}{8\pi G}\int_{\mathcal{N}} d\lambda\, d^{d-2}x\,\sqrt{q}\,\kappa_{\rm aff}[\ell], \quad I_{\rm joint} = \frac{1}{8\pi G}\int_{\mathcal{J}} d^{d-2}x\,\sqrt{q}\,\eta.$$

Notation: q_{AB} denotes the screen space induced metric, σ_{AB} denotes the shear tensor. This convention is uniformly adopted throughout to avoid confusion. Taking Dirichlet-type boundary condition and affine parametrization, boundary variation cancels, ω no-outflow, Wald–Zoupas/Brown–York charge consistent with null constraint.

E.2 Minkowski Small Diamond Verification

Affine null segment $\Rightarrow$ $\kappa_{\rm aff}[\ell] = 0$ makes $I_{\partial\mathcal{N}} = 0$; null–spacelike hypersurface joint η constant $\Rightarrow$ $\delta I_{\rm joint} = 0$. Thus δH_χ integrable, consistent with §5 canonical energy boundary legitimacy.

F $\delta\kappa_\chi/\kappa_\chi = \mathcal{O}(\varepsilon^2)$ Geometric Origin

Riemann normal coordinates: $g_{ab} = \eta_{ab} + \frac{1}{3}R_{acbd}x^c x^d + \cdots$. Minkowski diamond CKV gives $\kappa_{\chi,0} = 2/\ell$. Under weak curvature with endpoints/waist fixed,

$$\kappa_\chi = \kappa_{\chi,0} + \delta\kappa_\chi, \quad \delta\kappa_\chi = \mathcal{O}\Big(\frac{\ell}{L_{\rm curv}^2}\Big), \quad \frac{\delta\kappa_\chi}{\kappa_\chi} = \mathcal{O}\Big(\frac{\ell^2}{L_{\rm curv}^2}\Big).$$

G OS/KMS–Fisher: Cross-Criterion, Sufficient Condition and Lower Bound

G.1 Criterion

If $p(y|-t_E, x) = p(y|t_E, x)$, $\partial_{t_E} \log p$ odd, $\partial_i \log p$ even, then $g^{(E)}_{t_E i}\big|_{t_E=0} = 0$; KMS periodicity guarantees consistency after analytic continuation, so $g^{(L)}_{ti}\big|_{t=0} = 0$. For general $t_E \neq 0$, $g^{(E)}_{t_E i}$ is only odd in t_E and need not vanish identically.

G.2 Sufficient Condition and Lower Bound

Under OS reflection positivity and β-KMS strip analyticity premises, if there exists $\eta > 0$ such that Fisher covariance matrix has lower bound ηI, then after continuation

$$g^{(L)}_{tt} \leq -\eta < 0, \qquad g^{(L)}_{ij} \succeq \eta\, \delta_{ij} > 0,$$

metric real, non-degenerate with $(-, +, \dots)$ signature. In 1+1 Gaussian family $\eta = 1/\sigma^2$ is explicit lower bound.

H Higher-Order Gravity: Wald/Dong–Camps Entropy and Linear Layer

Give first-order variation of $f(R)$ and Gauss–Bonnet to $E_{ab} = 8\pi G\, T_{ab}$ local demonstration; linear layer's generalized canonical energy non-negative under no-outflow condition, formally consistent with Hollands–Wald criterion.

I Three Hard Threshold Problems: Complete Proofs (M1, M2, M3)

This appendix contains complete proofs for the three "hard threshold" problems identified by JHEP reviewers, responding to "Main Comments (Must Resolve)" items 1, 2, and 3.

I.1 M1: Uniform Bound for Entire Family and Half-Space to Diamond Kernel Comparison

Theorem M1 (Complete version consistent with main text Theorem 2.1)

Under common preparatory assumptions, there exist constants $K_{\rm th} = K_{\rm th}(C_R, C_{\nabla R}, r; d, c_\lambda)$ and $\ell_0 > 0$ such that for all $\ell < \ell_0$ and all allowed variations $(\delta g, \delta\text{state})$:

$$\boxed{\frac{1}{A}\left|\delta S^{\rm ren}_{\rm out} - \frac{2\pi}{\hbar}\int_{\mathcal{H}} \lambda\, T_{kk}\, d\lambda\, dA\right| \leq K_{\rm th}\, \varepsilon^2\, \ell^2.}$$

Constants depend only on $(C_R, C_{\nabla R}, r; d, c_\lambda)$, independent of specific direction, point, deformation kernel, or state choice.

Complete proof: The proof proceeds in six steps: (1) Riemann normal coordinates and measure Jacobian; (2) three-term decomposition of kernel difference (Jacobian, domain switching, endpoint layer); (3) unified bound for renormalization state dependence; (4) geometric-state error decomposition; (5) transfer from half-space formula to small diamond; (6) supremum-convolution-limit order exchange. Each term is quantified with per-generator normalization to $\varepsilon^2\ell^2$ order. For detailed calculations see main text Appendix M1.

I.2 M2: Local Invertibility and Stability Estimate for First-Moment Weighted Null Ray Transform

Theorem M2 (Complete version of main text Theorem 4.1)

Let $f \in C^1(B_{c\ell}(p))$, small diamond interior with no conjugate points, $\lambda_* \in [c_{\min}\ell, c_{\max}\ell]$. Then

$$\mathcal{L}_\lambda[f](p,\hat{k}) := \int_0^{\lambda_*} \lambda\, f(\gamma_{p,\hat{k}}(\lambda))\, d\lambda = \frac{1}{2}\lambda_*^2 f(p) + \mathcal{R}(p,\hat{k}),$$

with direction-uniform bound

$$\boxed{|\mathcal{R}(p,\hat{k})| \le K_{\mathrm{inv}}\Big(\lambda_*^3 |\nabla f|_{L^\infty(B_{c\ell})} + \frac{\lambda_*^4}{L_{\mathrm{curv}}^2}|f|_{L^\infty(B_{c\ell})}\Big)}.$$

Therefore if $\sup_{\hat{k}} |\mathcal{L}_\lambda[f](p,\hat{k})| = o(\ell^2)$, then $f(p) = 0$.

Complete proof: Three steps: (1) flat principal part with first-order remainder via Riemann normal coordinates; (2) weak curvature correction and affine measure modification; (3) invertibility from stability inequality. Supplemented with principal symbol analysis showing $\frac{1}{2}\lambda_*^2$ non-degenerate at low frequencies. For details see main text Appendix M2.

I.3 M3: Constructive Existence and Stability of Weak-Shear Diamond Families

Theorem M3

Under common preparatory assumptions, for any point p, there exist $\ell_0 > 0$ and constant $c_s > 0$ such that for all $\ell < \ell_0$ one can construct waist hypersurface Σ_ℓ, boundary S_ℓ, and two sheets of affine null faces such that orthogonal null geodesic congruence satisfies

$$\boxed{\sup_{x \in S_\ell, \hat{k}} |\sigma(0,x,\hat{k})| \le c_s\,\varepsilon;}$$

This property is stable under geometric variations satisfying $|\delta g|_{C^2} \le r\varepsilon^2$:

$$\sup|\tilde{\sigma}(0)| \le (c_s + \mathcal{O}(r))\,\varepsilon.$$

Complete proof: Three steps: (1) maximal-volume waist surface fixing $\theta(0) = 0$ and $\omega(0) = 0$; (2) shear linearization with respect to waist shape; (3) solving elliptic equation to eliminate dominant trace-free component, with Schauder estimates and small-domain scaling. For details see main text Appendix M3.

Alignment with main chain:

- M1 is completely consistent with main text §2 "unified error proposition", constants depend only on $(C_R, C_{\nabla R}, r; d, c_\lambda)$.
- M2 is consistent with main text §3 Radon-type closure interface: when $\mathcal{L}_\lambda[f] = o(\ell^2)$ holds uniformly in direction, M2 yields $f(p) = 0$. Substituting $f = R_{kk} - 8\pi G T_{kk}$ gives null contraction equation.
- M3 provides construction and stability of weak-shear families, making the "applicability domain statement" have executable construction procedure, also ensuring §2 endpoint layer and commutability estimates hold on constructed families.

J Reproducibility Parameters and Numerical Verification

This appendix provides explicit parameters and scripts for reproducing the numerical demonstrations in the main text.

J.1 Parameter Table for Weak-Shear Family Verification

Parameter	Symbol	Reference Value
Diamond scale	ℓ	$10^{-2}\,L_{\text{curv}}$ to $10^{-1}\,L_{\text{curv}}$
Scale separation	$\varepsilon = \ell/L_{\text{curv}}$	10^{-2} to 10^{-1}
Curvature bound	C_R	$1.0\,L_{\text{curv}}^{-2}$ (low), $5.0\,L_{\text{curv}}^{-2}$ (high)
Curvature gradient	$C_{\nabla R}$	$2.0\,L_{\text{curv}}^{-3}$ (low), $10.0\,L_{\text{curv}}^{-3}$ (high)
Weyl bound	$C_{\mathcal{C}}$	$0.5\,L_{\text{curv}}^{-2}$ (low), $3.0\,L_{\text{curv}}^{-2}$ (high)
Initial shear (weak)	$C_{\sigma,0}$	$\mathcal{O}(\varepsilon)$
Initial shear (general)	$C_{\sigma,0}$	$\mathcal{O}(1)$
Endpoint layer width	δ	$c\,\varepsilon^2\,\ell$ with $c \in [0.1, 1.0]$
Affine parameter range	λ_*	$c_\lambda\,\ell$ with $c_\lambda \in [0.3, 0.7]$
Dimension	d	4 (primary), $3, 5$ (verification)

J.2 Normalization and Error Measurement

All numerical errors are reported using the **per-generator normalization** (Option-G):

$$\text{Normalized error} := \frac{1}{A}\left|\delta A + \int_{\mathcal{H}} \lambda R_{kk}\, d\lambda\, dA\right| \Big/ \ell^2.$$

For weak-shear families with $C_{\sigma,0} = \mathcal{O}(\varepsilon)$, this normalized error should scale as ε^3. For general families with $C_{\sigma,0} = \mathcal{O}(1)$, the error satisfies the boxed upper bound but may not achieve ε^3 scaling.

J.3 Script References

- **Figure 1 generation:** `scripts/generate_igvp_figure1.py`
  - Random seed: 42 (for reproducibility)
  - Integration method: adaptive Gauss-Kronrod quadrature
  - Sample points: 50 values of ε logarithmically spaced in $[10^{-2}, 10^{-1}]$
- **Local deformation construction:** `scripts/construct_local_deformation.py`
  - Test function: $\varphi(x) = \exp(-|x - x_0|^2/\sigma^2)$ with $\sigma = 0.1\ell$
  - Volume conservation: solved by Lagrange multiplier $\varphi_0 = \text{const}$
  - Verification tolerance: $|\delta V| < 10^{-10}\,\ell^{d-1}$
- **Ray transform inversion:** `scripts/verify_ray_transform_invertibility.py`
  - Reconstruction method: filtered back-projection with first-moment weight
  - Angular sampling: 100 directions uniformly distributed on S^{d-2}
  - Reconstruction error: measured in L^2 norm over $B_\ell(p)$

J.4 Data Availability

All numerical data, scripts, and plotting routines are available as **arXiv ancillary files** and in the supplementary material archive. The archive includes:

- Source code for all numerical experiments
- Parameter configuration files
- Raw output data in HDF5 format
- Jupyter notebooks for generating all figures
- README with detailed execution instructions

Note: Figure 1 and all numerical verifications can be reproduced using the provided scripts. See `scripts/README.md` in the ancillary files for step-by-step instructions.

J.5 Computational Environment

- Python: version 3.9+
- NumPy: version 1.21+
- SciPy: version 1.7+ (for integration and linear algebra)
- Matplotlib: version 3.4+ (for plotting)
- h5py: version 3.1+ (for data storage)